SOLAR THERMAL AND WIND ENERGY APPLICATIONS Case Study of a Small Spanish Village

by

Christos S. IOAKIMIDIS [*]***, Sesil KOUTRA, Ali BAGHERI, and Konstantinos N. GENIKOMSAKIS***

European Research Area (ERA), Net-Zero Energy Efficiency in City Districts (NZED) Unit
Research Institute for Energy, University of Mons, Mons, Belgium

Original scientific paper
https://doi.org/10.2298/TSCI171229269I

The present work examines the supply of heating and electricity to the Spanish village of Uruena, using biomass and other local renewable sources as a result of the growing interest worldwide towards the development of sustainable and energy independent small communities. Specifically, this case study considers the design of a district heating system consisting of a solar heating plant, a biomass plant using straw as a sustainable fuel for the base load and an oil boiler for the peak load, coupled with a hot water tank as a thermal energy storage option. Two alternative scenarios are analyzed for electricity generation purposes, namely a system consisting of three small wind turbines and a system with a single large wind turbine. The results show that the cost of large-scale electricity storage depends on the application and often involves significant capital investments.

Key words: *biomass, district heating, solar thermal collectors, sustainable village, wind turbines*

Introduction

Recently, there have been increasing concerns regarding the potential consequences of global warming and climate change [1]. Thus, supply chain managers are now in search of some strategies to ensure not only profit maximization but also to reduce GHG emissions [2]. However, energy planning at the village level involves the application of decentralized planning principle [3]. In addition, experimental investigations show that the impact of fuel (ultralow sulfur light fuel) combustion characteristics on NO_x and GHG emissions are still a big concern [4]. Thus, there is a renewed interest in the development of sustainable and energy independent communities [5] starting from the level of individual villages that represent the smallest formations of organized energy consumption [3]. Agarwal *et al.* [6] tackled this problem with a multi-objective optimization model to calculate the best size of grid-independent solar-diesel battery-based hybrid energy system. In other studies, a hybrid biomass/wind/PV is considered [7] as a decentralized energy service for rural areas. Nevertheless, a discussion on a decision support analysis and life cycle thinking approaches are identical [8].

In this context, concerns about the environmental impacts of combustion processes encouraged studies on biomass fuels in order to reduce harmful emissions to the environment [9]. In addition, income and prices are among the main determinants of household energy

* Corresponding author; e-mail: christos.ioakeimidis@umons.ac.be

consumption [10]. Damette *et al.* [11] describe a theoretical framework to investigate households' energy consumption factors and highlight the motivations towards less polluting sources, including their environmental preference. Furthermore, for future electricity systems, the main challenge is to match the available electricity from variable renewable resources [12]. According to Le Truong *et al*. [13], the technical progress and changing consumed fuels in the building sector indicate that although energy consumption significantly grows up till 2050 the energy intensity remains at a reasonable level.

Moreover, Blum *et al.* [8] studied the levelized cost of electricity of solar photovoltaic (PV) and concluded that micro-hydro powered village grids are more competitive than diesel powered solutions. In addition, Huang *et al.* [14] claim that biomass energy plays an important role for energy conservation and environmental issues, although other aspects related to systems efficiency, secondary pollution, and process economics, are still crucial problems. In general, biogas and PV electricity generation for domestic applications have attracted more users as compared to other options [15].

Sustainable development and energy independence are two distinct terms that have been used interchangeably. An energy independent community can be achieved with revising the role and potential of rural areas. On the other hand, the economic crises have affected energy and primary commodity prices, which put more pressure on household budgets and often imply significant changes in various aspects of current lifestyle. Thus, the necessity of an integrated approach is evident, at the village level, to assist these small communities to efficiently use the full potential of their economic, social, cultural and environmental resources. In this context, the purpose of this work is to conduct a technical analysis for the supply of heating and electricity to the Spanish village of Uruena using biomass and other local renewable sources towards the development of a sustainable and energy independent small community considering economic issues. This case study examines the total energy consumption of the village in order to determine the capacities of the plants that need to be installed. Specifically, this work presents the design of a district heating system and the evolution of the total thermal load over the period of one year. Additionally, this work considers the use of a hot water tank for thermal energy storage and details the process of its dimensioning for two days of storage. Accordingly, the main contribution of this work is the techno-economic analysis of a small energy-independent community to cover thermal and electrical demand with locally available renewable resources and energy storage options.

Methods

This work conducts a techno-economic analysis of a small village for an energy-independent community. The study covers the analysis of the components of the district heating system, loads calculation, sizing the systems with the duration curve method for the solar heating collectors, sizing the thermal storage capacity, sizing the electric storage capacity, and electricity production with wind turbines.

Case study

In the context of this work, the small village of Uruena, Valladolid, Spain, serves as a case study towards the development of a small energy-independent community. The village is located in the region of Castile and Leon, in the northern half of the Iberian Peninsula, and according to the latest available studies, there are 224 inhabitants. The landscape characteristics and climatic conditions of the specific region indicate that, apart from biomass, wind and solar energy can also offer a potential technology solution to meet the total household energy needs. The village has a total of 160 houses, namely 96 one-floor and 64 two-floor houses. Ioakimidis *et al.* [16] consider two types of reference houses (one-floor and two-floor houses) to be used for load calculations, being a reasonable approximation of the structure of the actual houses. The one-floor houses have dimensions of 14 m × 7 m × 2.5 m and they include one 1 m × 2 m door and four 0.5 m × 0.7 m windows. Similarly, all two-floor houses include one door and eight windows. Moreover, it is assumed that the wall and floor thickness for both types of buildings are 0.65 m and 0.22 m, respectively [16].

Heat load calculations

The degree days are employed as typical indicators of building energy consumption for covering the space heating requirements. The calculation of heat consumption during the whole year is given by:

$$Q_{\mathrm{h,y}} = GD\, S_{\mathrm{d}} \frac{24}{1000} \tag{1}$$

$$S_{\mathrm{d}} = \frac{\varphi_{\mathrm{d}}}{t_{\mathrm{i}} - t_{\mathrm{d}}} \tag{2}$$

where GD is the number of degree-days in one year, S_{d} [WK^{-1}] – the specific design heat loss, φ_{d} [W] – the total thermal loss, t_{i} [K] – the indoor temperature, and t_{d} [K] – the design temperature.

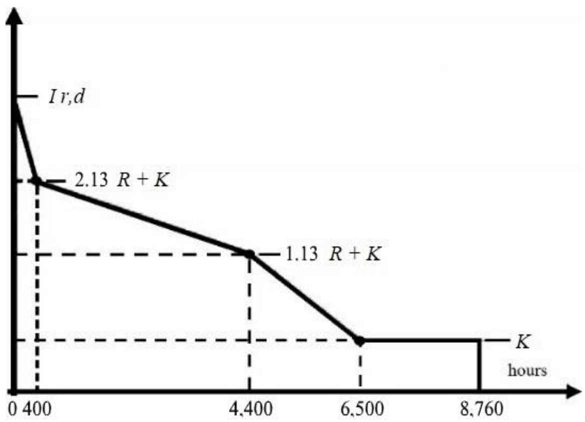

Figure 1. Duration curve according to required load

Duration curve approach

In this work, it is assumed that thermal energy loads are covered with a combination of a solar heating system, biomass and oil boilers. The corresponding capacities are determined using the duration curve approach [16]. The duration curve approach, as illustrated in fig. 1, relates the plant capacities with the operating hours in order to meet the requirements for the different loads during the year, such as summer load, base load and peak load. The determination of the characteristic points of the duration curve is based on the parameters R (space heating) and K (hot water and pipe losses) given in eqs. (3) and (4). The R [MW] represents the part of the consumption that changes during the year due to the outside ambient temperature (space heating), while K [MW] is the part of the consumption that is assumed to be constant during the year (hot water and pipe losses):

$$R = \frac{Q_{\mathrm{h,year}}}{3.6 \cdot 8760} \tag{3}$$

$$K = \frac{Q_{\mathrm{w,year}} + Q_{\mathrm{p,year}}}{3.6 \cdot 8760} \tag{4}$$

Solar thermal system

The calculations for the solar collectors are based on the *f*-chart method, which gives the annual fraction f_y [%] and the annual performance of the system Q_y [kWh per year]. Initially, a number of factors have to be determined using the eqs. (5)-(10):

$$F'U_L = a_1 + a_2(t_m - t_\alpha) \tag{5}$$

where F' is the collector efficiency factor, U_L [W°C^{-1}m^{-2}] – the overall heat loss transfer coefficient, $(t_m - t_a) = 40$ K – the temperature difference, and α_1 and α_2 are algebraic constants from the datasheet:

$$F'(\tau\alpha)_{en} = n_0 \tag{6}$$

where $(\tau\alpha)_{en}$ is the effective transmittance-absorptance product at 90° and n_0 is the efficiency when the temperature difference is 0 and F'' is the flow factor in which n is given by eq. (8):

$$F'' = \frac{1}{n}(1 - e^{-n}) \tag{7}$$

$$n = \frac{F'U_L}{q_m c_p} \tag{8}$$

In eq. (8) q_m is the mass-flow and c_p [Jkg^{-1}K^{-1}] – the specific heat capacity of the solar liquid:

$$F''' = [1 + F''n(\varepsilon^{-1} - 1)]^{-1} \tag{9}$$

where F''' is the heat exchanger efficiency factor and ε is calculated:

$$\varepsilon = 1 - \exp\left(-\frac{U_H A_H}{q_m c_p A_c}\right) \tag{10}$$

where A_c [m^2] is the area of the solar collector, U_H [WK^{-1}m^{-2}] – the overall heat transfer coefficient , A_H [m^2] – the area of the heating spiral. Next, the factor P that contains the absorbed solar radiation and factor Z of the heat loss of the solar collector are determined using eqs. (11) and (12), respectively:

$$P = A_c F''' F'' n_0 \frac{(\tau\alpha)_e}{(\tau\alpha)_{en}} \frac{H_s}{Q_{w,m}} \tag{11}$$

$$Z = A_c F' U_L F'' F''' (100 - t_a) \frac{\Delta\tau}{Q_{vem}} \tag{12}$$

where the ratio $(\tau\alpha)_e/(\tau\alpha)_{en}$ for a solar collector with one-layer equals 0.96, H_s – the solar radiation on a sloped surface with an inclination angle of 33°, t_a [°C] – the monthly mean temperature for ambient air, and $\Delta\tau$ – the number of hours per month. Having determined the parameters Z and P, the monthly fraction f_m is calculated:

$$f_m = 1.029P - 0.065Z - 0.245P^2 + 0.0018Z^2 + 0.0215P^3 \tag{13}$$

Then, the monthly heat performance Q_m is obtained from eq. (14). The annual heat performance Q_y is calculated by eq. (15). The annual fraction f_y is determined by eq. (16):

$$Q_{\mathrm{m}} = f_{\mathrm{m}} Q_{\mathrm{w,m}} \tag{14}$$

$$Q_{\mathrm{y}} = \sum_{1}^{12} Q_{\mathrm{m}} \tag{15}$$

$$f_{\mathrm{y}} = \frac{Q_{\mathrm{y}}}{\sum_{1}^{12} Q_{\mathrm{w,m}}} \tag{16}$$

Thermal energy storage

The thermal energy requirements for space heating on a monthly, $Q_{\mathrm{h,m}}$, and daily, $Q_{\mathrm{h,d}}$, basis can be calculated using eqs. (17) and (18) accordingly:

$$Q_{\mathrm{h,m}} = Q_{\mathrm{h,year}} \frac{GD_{\mathrm{m}}}{GD_{\mathrm{y}}} \tag{17}$$

$$Q_{\mathrm{h,d}} = \frac{Q_{\mathrm{h,m}}}{\text{number of days per month}} \tag{18}$$

Next, the total energy required for n days of thermal storage can be calculated: $Q_{\mathrm{a,nd}} = n \cdot Q_{\mathrm{a,d}} = n \cdot (Q_{\mathrm{wp,d}} + Q_{\mathrm{h,d}})$. Then, the volume of the hot water tank can be determined by solving eq. (19) for the volume V of the tank:

$$Q_{\mathrm{a,nd}} = \rho V c_p \Delta t \tag{19}$$

Electric energy storage

The storage options for high energy applications include batteries (*e. g.* sodium-sulphur, Li-ion, lead-acid), flywheels, pumped hydro and compressed air energy systems. Given that lead-acid batteries are considered as an established mature technology having a lower cost compared to other types of batteries [17], with the main disadvantages being the short life cycle and low depth of discharge. A rough estimation of the storage capacity needed for the system under study may be obtained from eq. (20):

$$\text{Capacity} = \frac{\text{Energy load per day} \times \text{Number of days for storage}}{\text{Voltage} \times \text{Efficiency}} \tag{20}$$

Wind turbine

The wind speeds at the surroundings of the village are analyzed using the Weibull distribution, expressed in eq. (21) as a statistic function that describes the probability density of the occurrence of a certain wind speed in the location under study [18]:

$$f(u) = \frac{k}{A}\left(\frac{u}{A}\right)^{k-1} \exp\left[\left(-\frac{u}{A}\right)^{k}\right] \tag{21}$$

where $f(u)$ is the probability density function of the wind speed, u – the wind speed, k – the shape factor, and A – the scale factor of the Weibull distribution. Taking into account the characteristic function, $p(u)$, of a wind turbine describes its output power with respect to wind speed, fig. 2(a). The mean power, P_{m}, is given in eq. (22). For simplicity reasons, it is assumed that the power curve may be approximated by three linear segments, as shown in fig. 2(b). The mean power output (in kW) can be calculated as in eq. (23):

$$P_m = \int_0 f(u)p(u)\mathrm{d}u \tag{22}$$

$$P_m = \frac{P_{max}}{\alpha_1 - \alpha_2}[G_k(\alpha_2) - G_k(\alpha_1) - e^{(-\alpha_3)^k}] \tag{23}$$

where P_{max} is the rated power, $\alpha_1 = u_1/A$, $\alpha_2 = u_2/A$, and $\alpha_3 = u_3/A$, while $G_k(\alpha) = (1/k)\gamma(1/k, \alpha^k)$ or be retrieved from auxiliary tables in [19]. At this point, it is noted that the exponential term in eq. (23) is often ignored because of its very low value. The annual electrical energy production, E_{ap}, can be calculated using $E_{ap} = P_m \cdot 365 \cdot 24$.

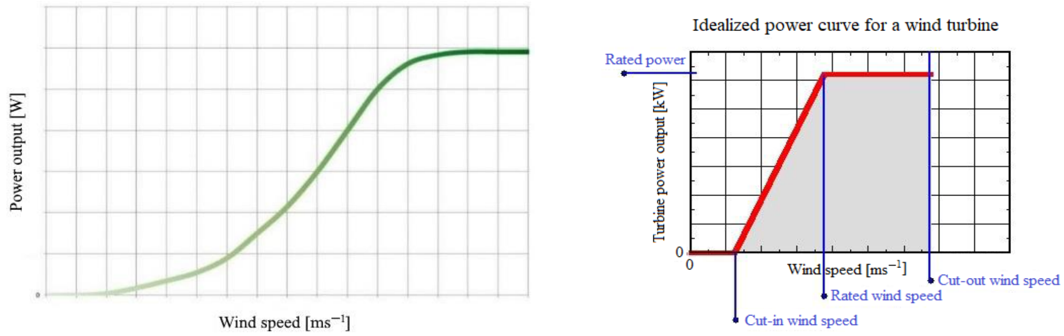

(a) **(b)**

Figure 2. Typical (a) and simplified (b) power curve of a wind turbine

Results

This section presents the results of the techno-economic analysis for the small village under study, covering aspects related to the district heating system, biomass and oil boilers, solar heating system, thermal and electrical storage, and wind turbines.

District heating system

A preliminary technical analysis presents the thermal losses, tab. 1, using a design temperature $t_d = -4$ °C, inside structure temperature $t_i = 20$ °C and ground temperature $t_{ground} = 15$ °C [16]. The re-insulation of the roof of a house with a layer of 10 cm of rockwool material would allow for savings of 4.7 kW in thermal losses, resulting in total thermal losses for the whole village equal to $\Phi_{tot} = 1224.2$ kW. The results on the losses for each section are cross-checked using with the Logstor calculator [20], which is a tool that can provide the loss in W/m for a section of pipe by knowing its length and diameter.

Table 1. Current thermal losses for one- and two-floor houses

Description	Notation	One-floor house	Two-floor house
Transmission losses	Φ_{tr} [W]	9684	13563
Ventilation losses	Φ_V [W]	590	1181
Linear losses	Φ_L [W]	290	310
Total thermal losses per house	Φ_d [W]	10564	15054
Total thermal losses for village	Φ_{tot} [kW]	1977.6	

The degree days for Uruena are 2142, as shown in tab. 2, while the annual consumption per one-floor house is $Q_{h,y1}$ = 12540 kWh per year = 45.2 GJ per year and per two-floor house is $Q_{h,y2}$ = 22160 kWh per year = 79.8 GJ per year. This results in a total annual heat consumption

Table 2. Average temperatures and degree-days for the village of Uruena

Month	Average daytime temperature [°C]	24-hour average temperature [°C]	Number of heating degree-days
Jan.	5.1	4.8	369
Feb.	6.9	5.9	309
Mar.	10.6	9.2	227
Apr.	12.1	10.6	183
May	15.9	14.5	52
June	21.5	19.6	7
July	23.2	21.4	1
Aug.	23.1	21.3	4
Sept.	19.5	17.7	65
Oct.	14.8	13.5	184
Nov.	8.8	7.8	349
Dec.	5.6	4.9	392
Year	13.9	12.6	2142

Figure 3. Map of the proposed pipe network

Table 3. Annual energy requirements for heating, hot water, pipe losses (left side) and values for duration curve (right side)

Space heating, hot water and pipe losses [GJ]		Hours	Capacity [MW]
$Q_{h,year}$	9440.4	0	1.0593 (= $\Phi_{r,d\ tot}$)
$Q_{w,year}$	481.1	400	0.6652 (= 2.13R + K)
$Q_{p,year}$	390.0	4400	0.3659 (= 1.13R + K)
Q_{tot}	10311.5	6500	0.0276 (= K)
		8760	0.0276 (= K)

$Q_{h,year} = 96Q_{h,y1} + 64Q_{h,y2} = 9440.4$ GJ per year. Furthermore, the estimated annual hot water consumption of the village is $Q_{w,year} = 481.1$ GJ, while the design of the pipe network in fig. 3 is proposed for distributing the hot water to the houses [16]. Moreover, the design capacity of the district heating system in order to cover the needs for space heating and hot water, as well as the thermal losses of the pipes, is $\Phi_{r,d\ tot} = 1.06$ MW.

Duration curve of annual thermal energy

Table 3 shows the annual thermal energy required for space heating, hot water and pipe losses and the pairs of coordinates of the characteristic points for the construction of the duration curve with parameters values $R = 0.299$ MW and $K = 0.0276$ MW. The total capacity required to cover the total thermal energy requirements of the village is divided into three parts, as shown in the initial duration curve in fig. 4a, the summer load will be covered with a solar heating system, the base load with a biomass plant while the peak load with an oil boiler [16].

Table 4 presents the resulting capacity and the annual heat supplied from each plant based on the initial duration curve. Given that a capacity of 60-70% of the maximum load is typically chosen for the biomass plant in district heating applications [21], a biomass plant of 65% of the total capacity is chosen. Table 4 also presents the revised values using the corrected duration curve shown in fig. 4(b).

Biomass and oil boilers

The results in tab. 4 are obtained by considering a biomass boiler based on the combustion of straw with the efficiency of $\eta = 0.85$ and net calorific value of $H_n = 4$ kWh/kg.

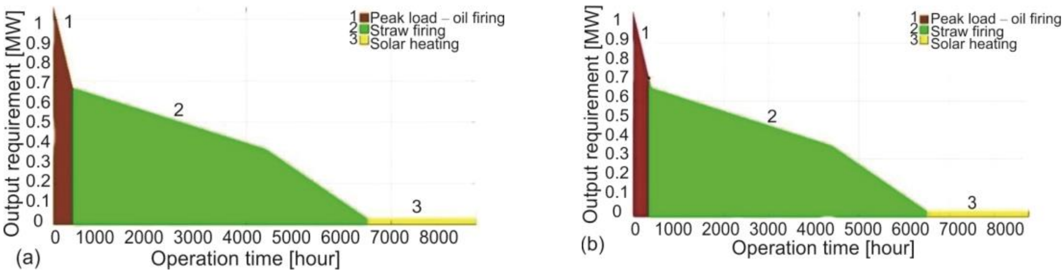

Figure 4. Initial duration curve (a); and (b) corrected duration curve

Table 4. Capacities and annual heat production based on initial (left side) and corrected (right side) duration curve

	Initial duration curve			Corrected duration curve		
	Oil boiler	Biomass plant	Solar heating	Oil boiler	Biomass plant	Solar heating
Capacity [MW]	0.394	0.6376	0.0276	0.343	0.689	0.0276
Capacity [%]	37.2	60.2	2.6	32.4	65.0	2.6
Production [MWh]	78.8	2562	242	59.4	2581	242

Moreover, it is considered that the biomass plant also serves as a backup option for the solar heating system. Therefore, the capacity of the biomass plant is:

$$\Phi_{b1} = \Phi_b + \Phi_s = 0.689 + 0.0276 = 0.716 \text{ MW}$$

while the corresponding annual amount of energy generated is:

$$Q_{y,b1} = Q_b + Q_s = 2581 + 242 = 2823 \text{ MWh.}$$

With the revised capacity of the biomass plant, the mass-flow of the straw will be $q_m = \Phi_{b1}/(\eta H_n) = 210.6$ kg/h, while the biomass required will be:

$$m_b = Q_{y,b1}/(\eta H_n) = 830286 \text{ kg per year.}$$

For the boiler, the home heating oil (often abbreviated as HHO) used has the density of ρ = 980 kg/m^3, the net calorific value of H_n = 10.9 kWh/L, and efficiency of η = 0.96. It follows that the volume flow of the oil is:

$$q_v = \Phi_{oil}/(\eta H_n) = 32.8 \text{ L per hours} = 0.033 \text{ m}^3 \text{ per hours,}$$

or equivalently in terms of mass-flow it is $q_m = q_v/\rho$ = 32.1 kg per hours. Accordingly, the annual mass of fuel (oil) needed is $m_{oil} = Q_{oil}/(\eta H_n)$ = 5.68 m^3 = 5562 kg. As a safety measure and for higher reliability reasons, another oil boiler is used as a backup having the same capacity of the biomass boiler, that is $\Phi_{boiler} = \Phi_{b1}$ = 0.716 MW, and it will have to cover a demand of $Q_{y,boiler} = Q_{y,b1}$ = 2823 MWh. For the backup oil boiler, the annual mass of fuel is:

$$m_{oil} = Q_{y,boiler}/(\eta H_n) = 269779.5 \text{ L} = 269.8 \text{ m}^3 = 264384 \text{ kg.}$$

Solar heating system

The thermal solar system provides the village with hot water supply during off-peak periods over the whole year, having a capacity of 27.6 kW in order to cover a requirement of 242 MWh. Table 5 presents the technical specifications of typical solar collectors, based on which a total of 43 units are required occupying a surface of about 432 m^2.

To determine the inclination angle of the collectors, an analysis of the solar radiation for the specific location of the village is made, tab. 6, based on data retrieved from the PV ge-

Table 5. Solar collector specifications

Characteristic	Value
Gross area [m^2]	10.05
Absorber area [m^2]	9.17
Collector capacity [L]	9
Mass-flow [kgm^{-2}s^{-1}]	0.005
Minimum collector incline [°]	25
Maximum collector incline [°]	75
Efficiency	0.804
Number of glass plates	4
α_1 [Wm^{-2}K^{-1}]	3.908
α_2 [Wm^{-2}K^{-1}]	0.011

Table 6. Monthly irradiation data

Month	Irradiation on optimally inclined plane [Wh/m^2/day]	Optimal inclination [°]	24 hours average of temperature [°C]
Jan.	2760	62	4.6
Feb.	3690	54	5.9
Mar.	5290	44	9.2
Apr.	5300	27	10.6
May	5970	14	14.5
June	6510	8	19.6
July	6730	12	21.4
Aug.	6550	24	21.3
Sept.	5670	39	17.7
Oct.	4330	51	13.5
Nov.	2910	59	7.8
Dec.	2040	61	4.9
Year	4820	33	12.6

Table 7. Monthly space heating consumption

Month	Days/month	GD_m	$Q_{h,m}$ [GJ]
Jan.	31	369	1776.350
Feb.	28	309	1487.512
Mar.	31	227	1092.768
Apr.	30	183	880.954
May	31	52	250.326
June	30	7	33.698
July	31	1	4.814
Aug.	31	4	19.256
Sept.	30	65	312.907
Oct.	31	184	885.768
Nov.	30	349	1680.071
Dec.	31	392	1887.071
Year	365	2142	10311.494

ographical information system – interactive maps (PVGIS) web service. The results obtained indicate that the optimal inclination angle for the solar collectors is 33°.

The heat transfer capacity rate $U_H A_H$ = 292 W/K is available from the datasheet of the hot water tank. After the necessary calculations, it follows that q_m = 0.0055 kgm^{-2}s^{-1}, $F'U_L$ = 3.468, $F'(\tau\alpha)_{en}$ = 0.804, F'' = 0.91, n = 0.068, F''' = 0.98, and ε = 0.77. Since there will be more than one solar collector in use, the term $U_H A_H$ is adjusted by the number of the solar collectors and the monthly energy needs $Q_{w,m}$ are obtained from eq. (24), assuming that the hot water consumption per inhabitant is 40 L per day:

$$Q_{w,m} = (0.95 + 0.0463\,B)n_d \qquad (24)$$

where B [day^{-1}] is the total consumption of hot water and n_d – the number of days per month. The space heating calculations are based on the total amount of heat required, the number of degree-days per month GD_m and per year GD_y. Indicatively, the heat required for January is $Q_{h,m} = Q_{tot}GD_m/GD_y$ = 1776.35 GJ, while the analytical results for each month are detailed in tab. 7.

The annual fraction f_y of the system is approximately 11%, as determined by eq. (17), implying that it is possible to consider a thermal storage option for a short period of time, which is assumed to be equal to two days in this work. The results show that the hot water demand of the village is covered, given that the requirement is 871.11 GJ and the supply 1253.61 GJ.

Thermal energy storage

A combi hot water tank is chosen as a thermal storage option for the district heating system, with sufficient capacity to cover the thermal needs for two days. To determine the capacity of the hot water tank, the annual hot water consumption $Q_{w,year}$ = 481.063 GJ, the pipe losses $Q_{p,year}$ = 390.047 GJ and the space heating requirements $Q_{h,year}$ = 9440.384 GJ, are taken into account. Hence, the average daily thermal energy demand for covering the hot water and pipe losses is $Q_{wp,d} = Q_{wp,year}/365 = 871.11/365 = 2.387$ GJ.

Next, the total energy required for two days of thermal storage can be calculated: $Q_{a,2d} = 2Q_{a,d} = 2(Q_{wp,d} + Q_{h,d})$. Table 8 details the relevant calculations for each month. Then, the volume of the hot water tank can be determined by solving eq. (19) for the volume V of the tank, where $\rho = 1005$ kg/m^3 is the density of the water, $c_p = 4.186$ kJ/kgK is the specific heat of the water and $\Delta t = 35$ °C is the temperature difference. Table 8 reveals that the average thermal energy requirement for two days over the whole year is similar to that of October, thus substituting the value for October as an average reference point in eq. (19), the volume of the hot water tank is almost $V = 420$ m^3.

Table 8. Daily thermal energy needs and requirements for two days of thermal storage

Month	Days/month	GD_m	$Q_{h,m}$ [GJ]	$Q_{h,d}$ [GJ]	$Q_{wp,d}$ [GJ]	$Q_{a,d}$ [GJ]	$Q_{a,2d}$ [GJ]
January	31	369	1776.350	57.302	2.387	59.688	119.376
February	28	309	1487.512	53.125	2.387	55.512	111.024
March	31	227	1092.768	35.251	2.387	37.637	75.274
April	30	183	880.954	29.365	2.387	31.752	63.503
May	31	52	250.326	8.075	2.387	10.462	20.923
June	30	7	33.698	1.123	2.387	3.510	7.020
July	31	1	4.814	0.155	2.387	2.542	5.084
August	31	4	19.256	0.621	2.387	3.008	6.016
September	30	65	312.907	10.430	2.387	12.817	25.634
October	31	184	885.768	28.573	2.387	30.960	61.920
November	30	349	1680.071	56.002	2.387	58.389	116.778
December	31	392	1887.071	60.873	2.387	63.260	126.520

Electric system

It is estimated that the electricity consumption per year for an average household is approximately 3071 kWh, hence the total annual electricity consumption for 160 houses in Uruena is assumed to be $E_{ac} = 3071 \times 160 = 491360$ kWh = 491.36 MWh. The village is located in a flat area that fosters the use of wind energy for electricity generation purposes. In this context, two alternative system configurations are analyzed, namely a system consisting of three small wind turbines and a system with a single large wind turbine, using the Wind Atlas methodology with detailed wind resource data for Europe [18].

System configuration with wind turbines

Assuming that the total electricity consumption in the village is divided into three parts and served by an equal number of identical wind turbines placed at different locations, the estimated rated power for each one of them is approximately 100 kW. For the purposes of this work, a wind turbine model with the power curve as in fig. 5(a) is chosen. According to the available technical specifications (Wind Energy Resources), the height of the hub is $h = 30$ m, fig. 5(b), the cut-in wind speed u_1 is 3 m/s and the wind speed at rated power u_2 is 12 m/s.

The value of the hub height is needed for evaluating the roughness class: this process consists in drawing a circle with the center at the installation point of the wind turbine and radius equal to 100 times the hub height (in this case 3 km), and then assigning a value of roughness for each one of the 12 sectors. Figure 6(a) shows the relative position of the installation point for the wind turbine 1 and the village of Uruena. The value of the roughness classes typically ranges from 1 to 5.

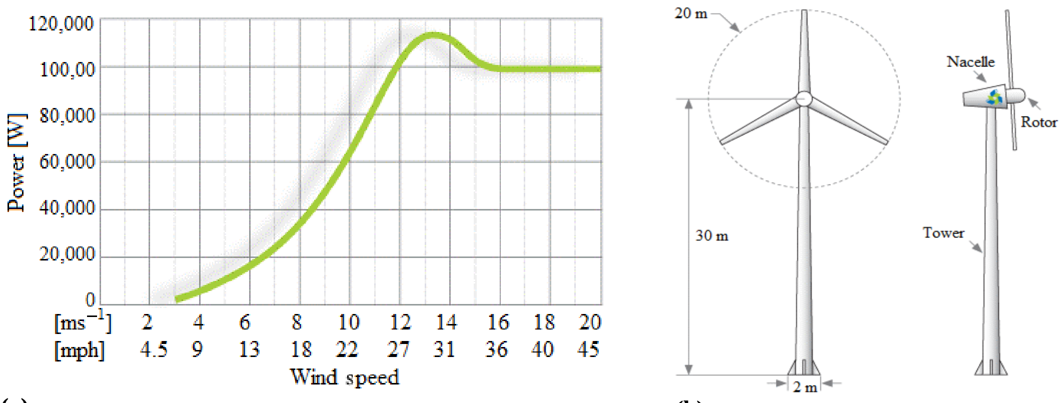

(a) (b)

Figure 5. Power curve (a); and design (b) of 100 kW wind turbine retrieved from (wind energy resources)

Table 9 shows the values of roughness chosen for each sector and the intermediate steps for calculating the parameters of the Weibull distribution for wind turbine 1, where the scale factor, A, and the shape factor, k, of the Weibull distribution, as well as the wind speed frequency, f, are retrieved from the statistical data available for the region under study [19]. Using the k value obtained, the values of $F_M(k) = \Gamma(1 + 1/k)$ and $F_u(k) = \Gamma(1 + 2/k)$ can also be retrieved from the available auxiliary tables in order to calculate the parameters $M = AF_M(k)$ and $u_2 = A^2F_\mathrm{u}(k)$, respectively. Then, the parameters f_M and f_u^2 are calculated as $fM/100$ and $fu^2/100$, respectively.

Given that the sum of the f values is not equal to 100, the following corrections apply:

$$M = f_M/(f/100) = 4.39,\ u^2 = f_u^2/(f/100) = 31.471, \text{ and } M^2/u^2 = 0.612$$

then, the new values of the Weibull parameters can be obtained:

$$k = F_k(0.612) = 1.264 \text{ and } A = MF_A(k) = 4.39F_A(1.264) = 4.724$$

given that $F_A(k) = 1/\Gamma(1+1/k)$. Next, the α parameters are obtained:

$$\alpha_1 = u_1/A = 3/4.724 = 0.635,\ \alpha_2 = u_2/A = 12/4.724 = 2.540,\ \alpha_2 - \alpha_1 = 1.905$$

in order to calculate $G_k(\alpha_1) = 0.503$ and $G_k(\alpha_2) = 0.905$. Using eq. (23) and $E_\mathrm{ap} = P_\mathrm{m}$ 365 24 with $P_\mathrm{max} = 100$ kW, the mean power output and annual energy production is $P_\mathrm{m1} = 21.1$ kW and $E_\mathrm{ap1} = 184.85$ MWh, respectively. The wind turbine 2 is considered to be installed in the south-west of the village of Uruena, as shown in fig. 6(b), while the corresponding calculations are the same as in the case of turbine 1. After the required corrections, given that the f values do not sum to 100, the mean power output and annual energy production for this wind turbine are $P_\mathrm{m2} = 17.9$ kW and $E_\mathrm{ap2} = 156.93$ MWh respectively. For wind turbine 3, the installation point chosen is in the west of the village, as indicated in fig. 6(c). Following the same process, as in the previous cases, the mean power output and annual energy production for this wind turbine are $P_\mathrm{m3} = 20.1$ kW and $E_\mathrm{ap3} = 175.68$ MWh, respectively. Overall, the energy produced on a yearly basis by the three wind turbines is:

$$E_\mathrm{ap1} + E_\mathrm{ap2} + E_\mathrm{ap3} = 517.46 \text{ MWh}$$

fully covering the total consumption in the village and producing a surplus of 26.1 MWh, given that the total consumption is 491.36 MWh.

Table 9. Parameters of Weibull distribution for wind turbine 1 (*h* = 30 m)

Sector	Roughness class	A	k	f	$F_M(k)$	M	$F_u(k)$	u^2	f_M	f_u^2
1	1	2.8	1.07	5.5	0.974	2.727	1.779	13.947	0.150	0.767
2	1	4	1.33	8	0.919	3.676	1.333	21.328	0.294	1.706
3	1	4.8	1.67	12.4	0.893	4.286	1.100	25.344	0.532	3.143
4	2	3.1	1.28	8.4	0.927	2.874	1.390	13.358	0.241	1.122
5	2	1.6	0.84	4.4	1.000	1.600	2.000	5.120	0.070	0.225
6	2	1	0.76	3.6	1.000	1.000	2.000	2.000	0.036	0.072
7	1	2.9	1.04	5.6	0.984	2.854	1.865	15.685	0.160	0.878
8	1	6.6	1.46	9.6	0.906	5.980	1.218	53.056	0.574	5.093
9	1	7	1.63	11.8	0.895	6.265	1.118	54.782	0.739	6.464
10	1	6.9	1.83	14.5	0.889	6.134	1.043	49.657	0.889	7.200
11	1	5.9	1.69	9.9	0.893	5.269	1.092	38.013	0.522	3.763
12	2	2.6	1.01	5.2	0.996	2.590	1.964	13.277	0.135	0.690
Sum				98.9					4.342	31.125

To supply all the electrical energy needed with one single wind turbine, a model with a nominal power output of at least 300 kW is required. Preliminary calculations with a 300 kW wind turbine showed that the annual electricity production is insufficient to cover the consumption of the village. Therefore, a wind turbine with 400 kW rated power is chosen with the following characteristics (Turbowind Energy: Turbowinds T400-34): h = 28 m, u_1 = 3 m/s and u_2 = 14 m/s.

(a) **(b)** **(c)**

Figure 6. Roughness circle for: (a) wind turbine 1; (b) wind turbine 2, and (c) wind turbine 3

Electricity storage and backup generator

Assuming three days of storage, 12 V voltage and an average efficiency of 85%, the estimated required capacity would be *Capacity* = 395.939 kAh, according to eq. (24). For a typical lead-acid model with 12 V voltage and 210 Ah capacity, the number of the batteries required for the system under study would be n = 395.939/210 ≈ 1886. With the unit price of this battery at 539.99 €, the resulting total cost is 1017900 €. The rated capacity of a backup generator required can be approximated as $P_{\text{generator}}$ = Daily consumption/24 hours = 1346.2 kWh/24 hours ≈ 60 kW. As an indicative example, the market price of a generator for this purpose is 11550 €.

Discussion

The operation of the district heating plant is based on a combination of generation technologies, namely solar power, oil and biomass. By definition, solar power is clean and pollution-free, while the combustion of biomass is typically considered to be carbon neutral. Considering that butane bottles are currently used for heating purposes in the houses of the village and combining the fact that the oil boiler of the designed district heating system is only used for the peak load, the proposed system configuration significantly contributes to the mitigation of GHG emissions. Moreover, the district heating plant is coupled with a hot water storage tank that can cover the thermal needs of the village for two *average* days, reducing thus the need for operating the oil boilers (either peak or back-up).

Alternative system configurations based on wind turbines are examined for electricity generation purposes, contributing to additional reductions in CO_2 emissions. From an economic point of view, the cost of a single 400 kW wind turbine is roughly estimated to be 480000 €, considering an average cost per kW of 1200 €. Under this assumption, the system with three 100 kW wind turbines would cost 360000 €, however, in this case, higher installation costs are incurred. Moreover, the installation and operation of large wind turbines are often connected to problems of visual, noise and environmental impact, which have serious implications on their social acceptance. In this context, the selection of a system with only one wind turbine, instead of a system with three identical wind turbines of similar size with the former one, appears to be a more suitable solution that could strike a reasonable balance between the social issues and the potential benefits. According to the techno-economic data presented in the previous section, it becomes obvious that the initial cost investment required for implementation of an energy system with electricity storage capabilities and a backup generator can be prohibitively high. Alternatively, a lower cost solution, yet more energy dependent, would be the implementation of a grid-connected system, where electricity can be bought directly from the grid if and when needed, while the surplus energy can be sold back to the grid.

Conclusion

This paper presented a detailed analysis for covering the thermal and electrical needs of the small Spanish village of Uruena using primarily biomass, as well as wind and solar energy, as a case study towards the development of a sustainable and less energy dependent small community. In technical terms, the systems include both electricity and thermal energy storage because of the intermittent nature of the RES, while special care is taken in order to incorporate backup boilers into the system to ensure the continuous energy supply to the village, even in the cases of system failures or non-favorable climatic conditions for considerable periods of time. For reasons of economy of space, a brief qualitative approach is employed to assess the environmental benefits in terms of CO_2 emissions reduction, while only selected economic data are presented to highlight some important cost factors for the implementation of the electric system with battery storage. These data also point to the fact that the cost of large-scale electricity storage depends on the application and often involves significant capital investments, partially explaining the lack of private sector initiatives in such applications and indicating that strong policy measures and action plans are needed at national and international level in order to revise the role and potential of rural areas.

Acknowledgment

This work has received funding from the European Commission under the RESIZED (Research Excellence for Solutions and Implementation of Net Zero Energy City Districts) project, as part of Grant Agreement No. 621408.

References

[1] Langbroek, M., *et al*., Learning from the Social Impacts Associated with Initiating a Windfarm Near the Former Island of Urk, The Netherlands, *Impact Assessment and Project Appraisal*, *30* (2012), 3, pp. 167-178

[2] Modak, N. M., *et al*., Managing Green House Gas Emission Cost and Pricing Policies in a Two-Echelon Supply Chain, *CIRP Journal of Manufacturing Science and Technology*, *20* (2018), Jan., pp. 1-11
[3] Ojha, K., Need of Independent Rural Power Producers in India—An Overview, *Clean Technologies and Environmental Policy*, *12* (2010), 5, pp. 495-501
[4] Geng, P., *et al*., Experimental Investigation on NO_x and Green House Gas Emissions from a Marine Auxiliary Diesel Engine using Ultralow Sulfur Light Fuel, *Science of The Total Environment*, *572* (2016), Dec., pp. 467-475
[5] Clark Ii, W. W., *et al*., Agile Sustainable Communities: On-Site Renewable Energy Generation, *Utilities Policy*, *16* (2008), 4, pp. 262-274
[6] Agarwal, N., *et al*., Optimization of Grid Independent Hybrid PV-Diesel-Battery System for Power Generation in Remote Villages of Uttar Pradesh, India, *Energy for Sustainable Development*, *17* (2013), 3, pp. 210-219
[7] Balamurugan, P., *et al*., Optimal Scheduling and Operation of Hybrid Biomass/Wind/PV Energy System for Rural Areas, *International Journal of Energy Technology and Policy*, *7* (2009), 1, p. 113
[8] Blum, N. U., *et al*., Rural Electrification through Village Grids – Assessing the Cost Competitiveness of Isolated Renewable Energy Technologies in Indonesia, *Renewable and Sustainable Energy Reviews*, *22* (2013), June, pp. 482-496
[9] Bianco, A., *et al*., On the Energy Consumption Computation in Content Delivery Networks, *Sustainable Computing: Informatics and Systems*, *16* (2017), Dec., pp. 56-65
[10] Damette, O., *et al*., Households Energy Consumption and Transition Toward Cleaner Energy Sources, *Energy Policy*, *113* (2018), Feb., pp. 751-764
[11] Schweiger, G., *et al*., The Potential of Power-to-Heat in Swedish District Heating Systems, *Energy*, *137* (2017), Oct., pp. 661-669
[12] Jingcheng, S., *et al*., The Impact of Technical Progress and Fuel Switching on Building Sector's Decarbonization in China, *Energy Procedia*, *61* (2014), Jan., pp. 373-376
[13] Le Truong, N., *et al*., Effects of Energy Efficiency Measures in District-Heated Buildings on Energy Supply, *Energy*, *142* (2018), Jan., pp. 1114-1127
[14] Huang, H., *et al*., Energy from Biomass and Waste: Case Studies in China, *International Journal of Energy Technology and Policy*, *1* (2003), 4, p. 400
[15] Mathur, J., Energy Technologies for Rural Areas Decentralised Power Generation Through MARKAL Modelling: A Case Study, *International Journal of Energy Technology and Policy*, *5* (2007), 3, p. 355-365
[16] Ioakimidis, C. S., *et al*., The Use of District Heating on a Small Spanish village, *Proceedings*, 26th International Conference on Efficiency, Cost, Optimization, Simulation and Environmental Impact of Energy Systems, Guilin, China, 2013
[17] ***, Logstor Calculator, http://calc.logstor.com/login.aspx
[18] Lars, N., *et al*., *Straw for Energy Production Technology -Environment -Economy* (2nd ed.), Trojborg Bogtryk, Aarhus, Denmark, 1998
[19] Troen, I., Lundtang Petersen, E., *European Wind Atlas*, Technical University of Denmark, Roskilde, Denmark, 1989
[20] Manwell, J. F., *et al*., *Wind Energy Explained: Theory, Design and Application*, John Wiley & Sons, New York, USA, 2009
[21] ***, World Energy Council, World Energy Resources: E-Storage, 2016

Paper submitted: December 29, 2017
Paper revised: March 22, 2018
Paper accepted: March 23, 2018